DICTA2002: Digital Image Computing Techniques and Applications, 21-22 January 2002, Melbourne, Australia.

A hybrid opto-electronic method for real-time automatic verification of handwritten signatures

Jean-Baptiste Fasquel and Michel Bruynooghe
Photonics Systems Laboratory, Louis Pasteur University
Bld Sebastien Brant, 67400 Illkirch, France
fasquel@apia.u-strasbg.fr

Abstract

This paper proposes a hybrid opto-electronical method for real-time automatic verification of handwritten signatures. This method combines several statistical classifiers and consists in three steps being first the transformation of signatures, then their characterization and finally their classification. The first step consists in transforming the original signatures using the identity and four Gabor transforms. The second step consists in intercorrelating the transformed signatures of the learning database, for each transformation. Then, the authenticity of signatures is verified. For each image transform, the signatures are intercorrelated with the similarly transformed signatures of the learning database. Finally, the fusion of the decisions related to each transform is performed to improve the recognition rate of our verification system.

Gabor transforms and image intercorrelations can be carried out at a frame rate of 1kHz, when using high speed optical correlators. The statistical classifications and fusion of decisions are performed in real-time on a classical digital signal processor. The opto-electronic implementation of the proposed method has been simulated on a database of 800 handwritten signatures, taking into account the specific constraints of the optical implementation.

Satisfactory results have been obtained when combining the statistical classifiers based on the identity and Gabor transforms: for a tolerance false rejection rate of about 4%*, the false acceptation rate is of about* 1.43% *thanks to the fusion method instead of* 2.56% *when only considering the identity transformation.*

1. Introduction

Human handwritings are among the most complicated objects to recognize [13]. Handwritten signatures form a special class of handwriting in which legible letters or words may not be exhibited. Signatures remain one of today's most acceptable means of verifying document validity such as bank cheques. If the signature is found to be false, the cheque is considered as being false as well. With the huge amount of bank cheques, a manual verification of signatures is a tedious task to do. This justifies the need of a fast and automatic processing for the verification of handwritten signatures.

A signature verification system can be classified as either on-line or off-line. On-line systems employ an electronic pen and pad to acquire dynamic information like pressure and speed of writing, but suffer the need of special acquisition devices. In this paper, we consider an off-line signature verification system, in which the signatures are converted to electronic form using a scanner or a camera. Many techniques, such as geometric moments [13, 1], envelope characteristics [1] and energy measures through wavelet decomposition [13], have been tested. In 1997, Murshed and al. [10] compared several methods, showing the high degree of classification accuracy reached by the currently available automatic verification systems with a mean false rejection or acceptation rate of about 1 % to 5 %. Due to the fact that most of shape description techniques are time consuming, the trend is to develop two stages verification systems: the first stage consists in elimininating obvious forgery signatures, and the second stage deals with the verification of more complicated cases, as underlined by Sabourin [14].

The objective of this paper is to propose an original real-time method for the fast elimination of obvious forgery signatures. The proposed method, for this first stage, can be implemented on high speed optical correlators as those currently working at a frame rate higher than 1kHz [11, 5], to reduce the number of forgeries to be processed in the second stage. Preliminary tests have been carried out recently on a small database of 133 handwritten signatures and have shown the feasability and the potential of our approach [7]. Now, the aim is to perform a large scale evaluation using

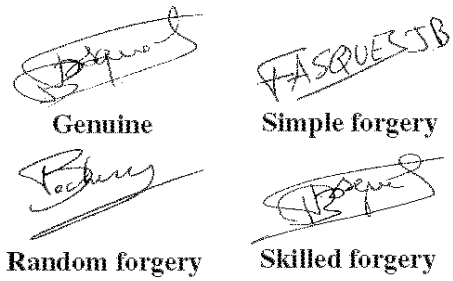

Figure 1: An example of the four kinds of handwritten signatures.

a database of 800 handwritten signatures. Moreover, this evaluation takes into account the specific constraints of the optical implementation.

In the second section, the specificity of the data is presented. In the third and fourth sections, the proposed verification method and its hybrid opto-electronic implementation are described. Simulation results are detailed in the fifth section.

2. Data

With respect to a given writer w_i, there are two kinds of handwritten signatures: the genuine signatures, and the forgeries written by other writers. Among forgeries, we typically consider [7, 12]:

- *Simple forgeries:* where the forger makes no attempt to simulate a genuine signature.
- *Random forgeries:* where the forger uses his/her own signature instead of trying to make an imitation.
- *Skilled forgeries:* where the forger tries and practices imitating as closely as possible the static and dynamic information of a signature.

The figure 1 gives an example of these four kinds of signatures. Murshed and al. [10] reported that most forgeries are random. This justifies the interest of the development of a two stages verification system, where the first stage deals with the rapid elimination of forgeries, being mostly random, and the second stage is used only for more complicated cases.

3. Method

The principle of the proposed verification method is illustrated by the figure 2. The signature o to be verified is presented to the verification system. A one-class approach has been used to check whether it has really been written by the writer w. The verification is performed by comparing the characteristics of the signature o with those of reference signatures $\{r_1, r_2, \ldots, r_n\}$ of the writer w. For this purpose, the signature o is preliminary transformed using the identity transform I and four Gabor filterings $\{G_1, G_2, G_3, G_4\}$ so as to enhance specific information. Gabor transforms allow to enhance the underlying structures of the signatures which are the most predominant strokes along several predefined orientations. This is justified by the fact that a signature is characterized by the position of its different strokes which are supposed to have a relatively constant width fixed by the pencil used for the acquisition.

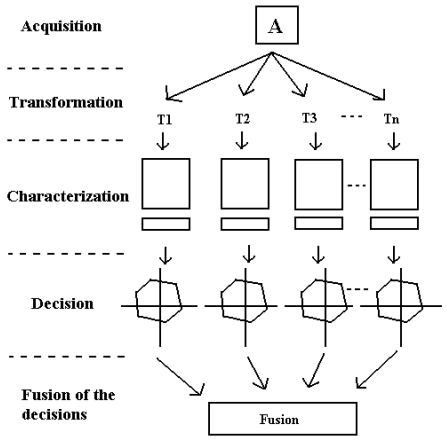

Figure 2: Principle of the proposed verification method for fast elimination of random forgeries.

Using these five transforms, the signature o to be verified is represented by the set $\{o_t | t \in T\}$ of transformed images, with $T = \{I, G_1, G_2, G_3, G_4\}$.

Then, for each transformation $t \in T$, the transformed signature o_t is characterized by intercorrelating it with each of the similarly transformed references $\{r_{t,1}, r_{t,2}, \ldots, r_{t,n}\}$. For each transformation $t \in T$, we decide whether the signature o to be verified really belongs to the writer w, by considering the intercorrelations $\{C(o_t, r_{t,i}) | i = 1, \ldots, n\}$. Finally, we make the fusion by intersection of the decisions taken for each transformation.

3.1. Gabor transforms

To enhance the constitutive strokes of signatures, we propose to use, as in our previous work [7], the Gabor wavelet filters whose real parts are useful tools for orientation and size sensitive object detection [3, 2]. The real part of the Gabor wavelet function is defined by $g(x, y)$:

$$g(x,y) = exp[-\pi((\frac{x^{'}}{\sigma_{x^{'}}})^2+(\frac{y^{'}}{\sigma_{y^{'}}})^2)]\times cos(2\pi(xu_0+yv_0)), \quad (1)$$

with $u_0 = fcos(\theta)$ and $v_0 = fsin(\theta)$, θ being the direction of propagation of the wavelet. $x^{'}$ and $y^{'}$ are defined by $x^{'} = xcos(\theta) + ysin(\theta)$ and $y^{'} = -xsin(\theta) + ycos(\theta)$. $\sigma_{x^{'}}$ and $\sigma_{y^{'}}$ are the standard deviation along the $x^{'}$ and $y^{'}$ axis in the θ rotated basis.

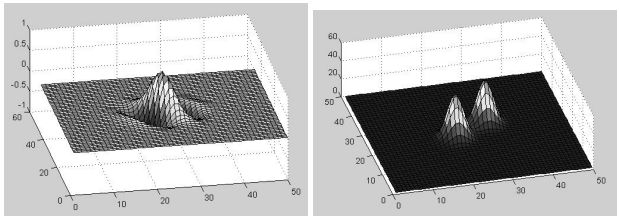

Figure 3: Example of Gabor filter in the spatial domain (left), and in the frequential domain (right).

The figure 3 displays an example of $g(x,y)$ and its related Fourier spectrum which is composed of two gaussian functions respectively centered at the rotated frequencies $(u_0^{'}, v_0^{'})$ and $(-u_0^{'}, -v_0^{'})$. The expression of the first gaussian is:

$$G(u,v) = exp[-\pi(u^{'} - u_0^{'})^2\sigma_{x^{'}}^2 - \pi(v^{'} - v_0^{'})^2\sigma_{y^{'}}^2)] \quad (2)$$

By tuning correctly the different parameters of the Gabor function, the detection of strokes having a specific width along a specific orientation can be optimized. The parameters to be defined are: the angle θ, the frequency f and the standard deviations $\sigma_{x^{'}}$ and $\sigma_{y^{'}}$.

Casasent [3] has shown that to detect an object of width d, the optimal values for f and $\sigma_{x^{'}}$ are: $f = \frac{1}{2d}$, and $\sigma_{x^{'}} = 2d$. The standard deviation $\sigma_{y^{'}}$ is linked to the angular step $\Delta\theta = \frac{\pi}{n}$, where n is the number of orientations chosen for the decomposition of the signatures ($n = 4$ in our case). To ensure the specificity of such a decomposition, the Gabor filters don't have to overlap. By taking into account this constraint, we finally find [7]:

$$\sigma_{y^{'}} = \frac{\sqrt{\frac{ln(2)}{2\pi}}}{f \times tan(\frac{\pi}{2n})}. \quad (3)$$

For each signature, the stroke width d has been estimated using classical morphological granulometry [6]. Then, the parameters of the four Gabor filterings have been automatically computed thanks to the previous formula.

3.2. Characterization by intercorrelation

For each transformation $t \in T = \{I, G_1, G_2, G_3, G_4\}$, the signature o to be verified is characterized by the vector v of normalized correlation peaks $\{C(o_t, r_{t,i})|i = 1, \ldots, n\}$, obtained by intercorrelating the considered signature with each of the similarly transformed references $\{r_{t,1}, r_{t,2}, \ldots, r_{t,n}\}$. Hence, the signature o to be verified is characterized by the n-dimensional feature vector v whose i^{th} component $C(o_t, r_{t,i})$ is theoretically defined by:

$$C(o_t, r_{t,i}) = \frac{max|\int\int o_t^*(\alpha,\beta) r_{t,i}(\alpha + x, \beta + y)\, d\alpha d\beta|}{E_{o_t} E_{r_{t,i}}}, \quad (4)$$

where E_{o_t} and $E_{r_{t,i}}$ are the energies of the corresponding transformed signatures.

3.3. Decision criterion and fusion

The verification of handwritten signatures is considered as a one-class classification problem, as assumed by Murshed and al. [10], because the only reliable knowledges are provided by the reference signatures belonging to a given writer.

For each transformation $t \in T$, the signature o to be verified is classified by comparing its feature vector with the n feature vectors related to the n reference signatures. These n feature vectors have been obtained by intercorrelating the n transformed references. This constitutes the learning step which leads to the obtention of the $n \times n$ correlation matrix M whose general term is $M_{i,j} = C(r_{t,i}, r_{t,j})$. The mean intercorrelation $\mu_{t,i}$ related to the row i is then computed:

$$\mu_{t,i} = \frac{1}{n-1} \sum_{j \neq i} C(r_{t,i}, r_{t,j}). \quad (5)$$

Finally, for each transformation, a minimum correlation threshold τ_t will then be defined by $\tau_t = \mu_t - k \times \sigma_t$, where μ_t and σ_t denote the mean and the standard deviation of the mean intercorrelation $\mu_{t,i}$. The optimal value of the parameter k can be experimentally estimated taking into account the compromise between false acceptations and false rejections. This ends the learning step.

For each transformation $t \in T$, the classification of the signature o to be verified is performed by computing the intercorrelations $\{C(o_t, r_{t,j})|j = 1, \ldots, n\}$, and estimating their mean value:

$$\mu_{o_t} = \frac{1}{n} \sum_{j=1}^{n} C(o_t, r_{t,j}). \quad (6)$$

Then, the signature o is rejected and considered as a forgery if μ_{o_t} does not belong to the previously defined minimum

correlation threshold τ_t. Hence, the result $\gamma_t(o)$ of the classification decision is defined by:

$$\gamma_t(o) = (\mu_{o_t} \geq \tau_t). \quad (7)$$

This ends the classification step with respect to the given transformation t.

Finally, the fusion of classifiers is performed by intersection : if a signature o to be verified is rejected with respect to at least one transformation, it is considered as a forgery.

4. Constraints of the optical implementation

The proposed optical processor is an optical correlator based on the Vander Lugt [15] architecture. Its principle is given by the figure 4. The input image is loaded on a spatial light modulator (SLM) in the input plane of the setup. The SLMs used in optical correlation are typically screens made of liquid crystals. The first lens carries out the Fourier transform of the input image. In the Fourier plane, there is a second spatial light modulator on which we load the Fourier transform of the filter. We recall that, in our case, the filters used are Gabor filters and Matched filters corresponding to the transformed reference signatures. Then, the Fourier transform of the input image and the Fourier transform of the filter are multiplied. The second lens performs a second Fourier transform of the previous spectrum product, leading to the correlation image in the output plane.

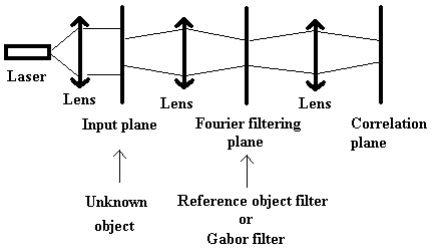

Figure 4: Principle of the Vander Lugt optical correlator.

To carry out the filterings at a frame rate of 1 kHz, the current technological limitations involve that the SLMs are binary SLMs made of ferro-electric liquid crystals. The current high speed CCD cameras enable the acquisition of Gabor filtered images and of correlation images at a frame rate of 1 kHz. We now describe the specific constraints involved by the use of these devices.

The optical implementation of the Gabor wavelet has been discussed by Li and al. [9] in 1992. Due to the dynamic of the high speed SLM used in the Fourier plane, only two grey-levels can be encoded instead of the fully complex function corresponding to the Gabor filter in the Fourier domain. Thus, the Gabor transform is implemented as an ideal bandpass filter obtained by thresholding, in the Fourier domain, the amplitude of the filter at 3db.

The optical implementation of the Gabor filtering presents a second drawback. In fact, Gabor filters are real valued filters, composed of positive and negative values. Thus, the filtered images contain both positive and negative values.

Due to the quadratic acquisition achieved by CCD detectors, the negative lobes become positive. Thus, by thresholding the optically Gabor filtered image, we detect some oriented linear segments of the signature surrounded by parallel side-lines corresponding to the response of the negative lobes of the Gabor filter. The figure 5 gives an example of a handwritten signature filtered by simulated Gabor filters.

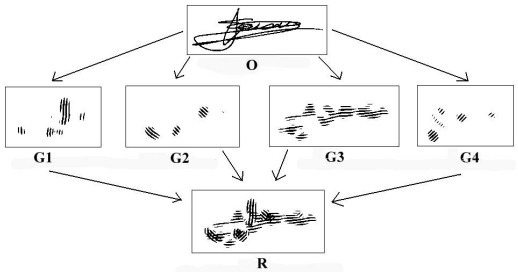

Figure 5: Simulation of the optical implementation of the Gabor filtering: example of the decomposition of a handwritten signature using four Gabor filters. **O:** Original handwritten signature. **G1, G2, G3, G4:** Gabor filterings of the original signature, at angle O, $\frac{\pi}{4}$, $\frac{\pi}{2}$ and $\frac{3\pi}{4}$. **R:** Reconstructed signature from the Gabor filterings.

As said previously, the fast SLM in the Fourier plane enables to encode only binary filters. Thus, for intercorrelations, the full complex matched filters must be reduced to binary filters. For matched filtering, we typically keep the phase information of the filter [8], which contains more information about the shape of the object than the amplitude [4]. By thresholding the phase of the filter, it is then possible to implement intercorrelations on the optical correlator. Such binary filters are the so-called Binary Phase Only Filters (BPOF) [8].

In the following section, we present results obtained by simulating the constraints of the optical implementation of the proposed verification method.

5. Simulation results

For simulation experiments, a database of 800 handwritten signatures was used. Such a database size is commonly encountered in the literature. To generate this database, 15

writers signed 50 times. For each writer, 25 handwritten signatures are used for learning and 25 for evaluating the false rejection rate (FRR). A database of 50 random forgeries is used to evaluate false acceptation rates (FARs). In

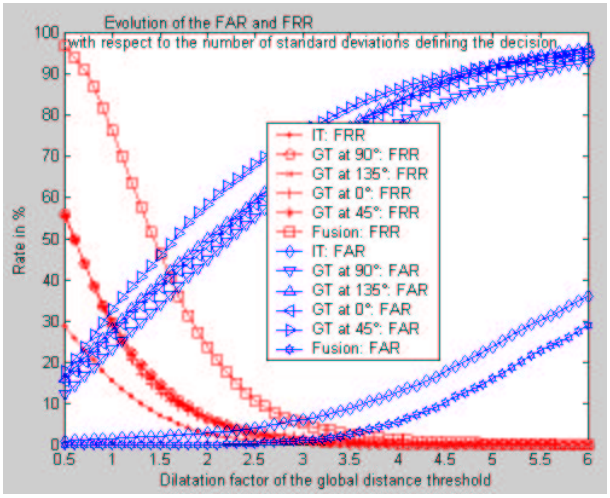

Figure 6: False acceptation and rejection rates (FAR and FRR) versus parameter k. These classification rates are given for each individual classifier based either on the identity transform (**ID**) or on Gabor transforms (**GT**), as well as for the fusion method.

our experiments, for a given writer and a given value of the parameter k, FRRs and FARs have been averaged over 100 random choices of 25 references chosen among the 50 available genuines signatures. These experiments have been carried out with k ranging from 0.5 to 6 by steps of 0.1. Such a large interval has been chosen for pedagogical reasons to fully illustrate the variations of FARs and FRRs with respect to k. Experimental results have confirmed that acceptable classification rates are obtained when k varies between about 2 and 4.

The figure 6 gives the variations of FARs and FRRs with respect to k, for each individual classifier based either on the identity transform or on Gabor transforms, as well as for the fusion method. The presented results have been averaged over the 15 writers. It is observed that the FRR decreases and the FAR increases when k increases, which is logical because we accept more and more signatures as correct, including both genuines and forgeries. We see that, below a given k value, the FRR of the fusion method is much higher than for any other transform. This is due to the fact that genuine signatures which are rejected by the fusion method are the union set of the genuine signatures rejected by each statistical classifier.

The figure 7 illustrates the variation of the FAR with respect to the FRR, for the individual classifier based on the

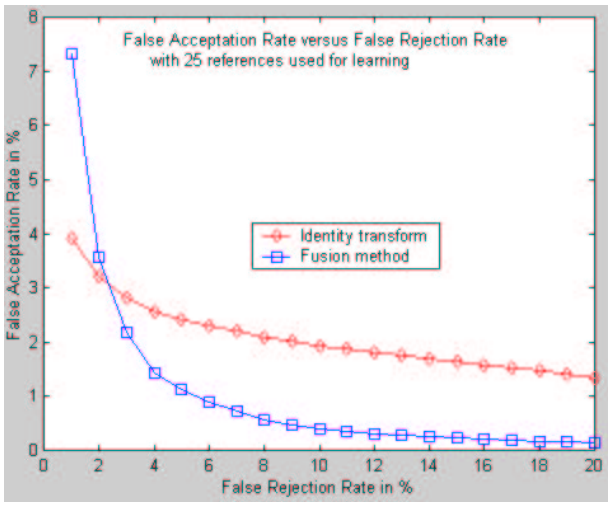

Figure 7: False acceptation rates versus the false rejection rates, averaged over the 15 writers.

identity transform and for the fusion of classifiers. The fusion of classifiers improves the FAR only above of certain FRR of about 2.5 % (as shown in table 1). This is due to the fact that to insure a low FRR for the fusion, we have to insure a low FRR for each image transform, taking a larger k.

FRR	0.5	1	2	2.5	3	4
IT: FAR	4.92	3.91	3.21	2.98	2.81	2.56
F: FAR	13.20	7.31	3.58	2.88	2.18	1.43

Table 1: False Acceptation Rates (FAR) obtained for different False Rejection Rates (FRR). Results are given in the case of the identity transformation (IT) and the fusion method (F).

As seen in table 1, for a false rejection rate of about 3% (resp. 4%), by only considering the classifier based on the identity transform, 2.81% (resp. 2.56%) of random forgeries are recognized as genuines. Thanks to the fusion method, this latter rate decreases from 2.81% (resp. 2.56%) down to 2.18% (resp. 1.43%).

The figure 8 gives some examples of signatures, and their transformed version, which have been analyzed by the proposed verification system. The line A and B of figure 8 show examples of genuine signatures. The lines C and D are two random forgeries which have been classified has genuines. Lines E and F present two random forgeries which have been eliminated with respect to only one transformation.

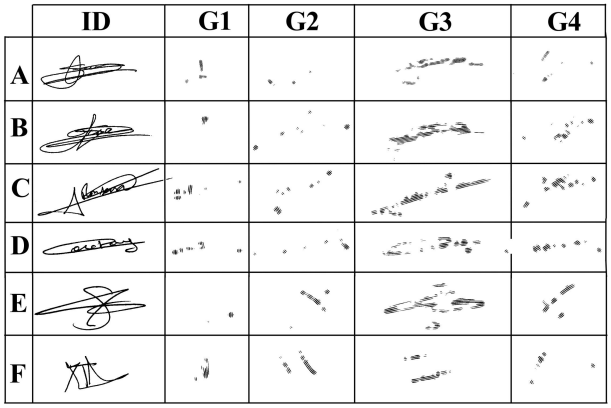

Figure 8: Examples of handwritten signatures which have been analyzed by the proposed system. The transformation are the identity transformation (ID), the Gabor transformation at angles O^o (G1), 45^o (G2), 90^o (G3), 135^o (G4). **A and B:** two genuines. **C and D:** two random forgeries classified as genuines. **E:** random forgery eliminated by ID only. **F:** random forgery eliminated by G2 only.

6. Conclusion

A hybrid opto-electronic method for the fast elimination of random forgeries has been proposed. This method is based on the characterization of handwritten signatures by their intercorrelations with a reference database. Such a charaterization has been applied for different transformations of the signatures including the identity transform and four Gabor transforms. Then, by carrying out the fusion of the decisions related to each transform, it was expected that false acceptation rate would decrease. This approach has the advantage of being optically implementable on the current high speed optical correlators. Nevertheless, such optical correlators have two major drawbacks being the small encoding dynamic of the filters and the quadratic acquisition of CCD cameras.

For these reasons, we have proposed to evaluate our approach by taking into account these two specific constraints. Simulation experiments have been carried out on a large database of 800 handwritten signatures, as usually done in the literature to validate a system for the verification of handwritten signatures.

These results validate the proposed approach. The hybrid opto-electronic implementation of this verification method would enable to test the authenticity of an unknown signature in about 125 ms (for 25 references), which is dramatically faster than with any digital processor. The next step will consist in carrying out these experiments on an optical correlator.

References

[1] R. Bajaj and S. Chaudhury. Signature verification using multiple neural classifiers. *Pattern Recognition*, 30(1):1–7, 1997.

[2] J. Cai and Z.-Q. Liu. Off-line unconstrainted handwritten word recognition. *International Journal of Pattern Recognition and Artificial Intelligence*, 14(3):259–280, 2000.

[3] D. P. Casasent and J.-S. Smokelin. Real, imaginary, and clutter gabor filter fusion for detection with redeuced false alarms. *Optical Engineering*, 33(7):2255–2263, July 1994.

[4] K. R. Castleman. *Digital Image Processing*. Prentice Hall, 1996.

[5] T.-H. Chao, H. Zhou, and G. Reyes. 512x512 high-speed grayscale optical correlator. *Proceedings of the SPIE: Optical pattern recognition XI*, 4043:40–45, 2000.

[6] Dougherty. *An introduction to morphological image processing*. Spie optical engineering press, 1992.

[7] J.-B. Fasquel, C. Stolz, and M. Bruynooghe. Real-time verification of handwritten signatures using a hybrid opto-electronical method. *2nd IEEE R8 - Eurasip Symposium on Image and Signal Processing and Analysis (ISPA'01)*, June 2001.

[8] B. V. K. V. Kumar and L. Hassebrook. Performance measures for correlation filters. *Applied Optics*, 29(20):2997–3006, 1990.

[9] Y. Li and Y. Zhang. Coherent optical processing of gabor and wavelet expansions of one- and two-dimensional signals. *Optical Engineering*, 31(9):1865–1885, September 1992.

[10] N. A. Murshed, R. Sabourin, and F. Bortolozzi. A cognitive approach to off-line signature verification. *International Journal of Pattern Recognition and Artificial Intelligence*, 11(5):801–825, 1997.

[11] M. J. O'Callaghan, D. J. Ward, S. H. Perlmutter, L. Ji, and C. M. Walker. A highly integrated single-chip optical correlator. *SPIE Algorithms, Devices and Systems for Optical Information Processing*, 1998.

[12] R. Plamondon and G. Lorette. Automatic signature verification and writer identification - the state of art. *Pattern Recognition*, 22(2):107–131, 1989.

[13] V. E. Ramesh and M. N. Murty. Off-line signature verification using genetically optimized weighted features. *Pattern Recognition*, 32:217–233, 1999.

[14] R. Sabourin, editor. *Off-line Signature Verification: Recent Advances and Perspectives*, Curitiba, Brazil, 1997. Proc. of the BSDIA'97. pp. 84-98.

[15] A. VanderLugt. Signal detection by complex spatial filtering. *IEEE Transactions on Information Theory*, IT-10:pp. 139–145, 1964.